

Triazole Cycloaddition as a General Route for Functionalization of Au Nanoparticles

David A. Fleming, Christopher J. Thode, and Mary Elizabeth Williams*

Department of Chemistry, The Pennsylvania State University, 104 Chemistry Building,
University Park, Pennsylvania 16802

Received January 21, 2006. Revised Manuscript Received March 5, 2006

Triazole formation by 1,3-dipolar cycloaddition reactions, “click” chemistry, has been used to functionalize the surfaces of Au nanoparticles. Au particle samples were first synthesized through standard procedures, the methyl-terminated chains partially exchanged with ω -bromo-functionalized thiol, and the Br termini converted to azides by reaction with NaN_3 . These particles were then reacted with a series of alkynyl derivatized small molecules in nonpolar solutions, which led to their attachment through the formation of a 1,2,3-triazole ring, confirmed through NMR and IR spectroscopies. Click reactions were used to impart chemical functionality to the Au particles, which is assessed using fluorescence spectroscopy and cyclic voltammetry.

Introduction

Functional nanomaterials designed to perform a specific reaction are of intense interest because of their potential uses in medical diagnostics,¹ drug delivery,² and catalysis.³ The majority of reports have sought to leverage the intrinsic physical properties of the nanomaterials, such as magnetic nanoparticles for high-density magnetic data storage,⁴ or noble-metal particles for nonlinear optics.^{1,5} Efforts aimed toward control and improvement of these properties have largely focused on modifications of the nanoparticle synthesis. Nanoparticle magnetic moments, for example, have been adjusted by careful modification of the chemical composition,^{4a,6} size, and crystal structure,^{4a} while the fluorescence emission wavelengths of semiconductor nanocrystals are known to be strongly dependent on particle size.⁷ An alternative approach is to impart chemical functionality to

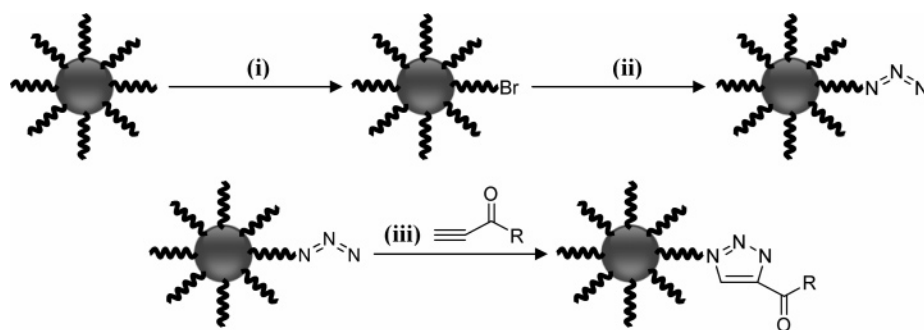
nanoparticles, and the most well-understood method is the use of place-exchange reactions that rely on displacement of surface ligands. The utility and generality of these reactions for the modification of Au nanoparticles was first described by Murray et al.,⁸ who produced chemically useful particles by replacement of the monolayer ligands with ω -functionalized alkanethiols.

A significant drawback to this method is the need to synthesize individual thiolated ligands for insertion into the monolayer. The inclusion and tailoring of functional moieties has long been a goal in small-molecule organic chemistry, and as a result an enormous number of reactions have been developed to convert, for example, alcohols into carboxylic acids and halides into alkenes,⁹ or to link molecular species using amide or ester condensation chemistry.¹⁰ These reactions have all been applied for the modification of Au nanoparticles' surface structure and chemistry.¹¹ However, these chemistries are not always compatible with the desired applications so that the development of additional, general routes toward nanoparticle functionalization is still necessary for their use in emerging nanotechnologies.

Molecular species can be linked by 1,3-dipolar cycloaddition reactions,¹² which were first described by Huisgen¹³ and have recently gained renewed attention with the advent of “click” chemistry. In this latter method, azide-containing

* Corresponding author. E-mail: mbw@chem.psu.edu.

- (1) (a) Haes, A. J.; Hall, W. P.; Chang, L.; Klein, W. L.; Van Duyne, R. P. *Nano Lett.* **2004**, *4*, 1029. (b) Haes, A. J.; Chang, L.; Klein, W. L.; Van Duyne, R. P. *J. Am. Chem. Soc.* **2005**, *127*, 2264. (c) El-Sayed, I. H.; Huang, X.; El-Sayed, M. A. *Nano Lett.* **2005**, *5*, 829.
- (2) (a) Gupta, A. K.; Gupta, M. *Biomaterials* **2005**, *26*, 3995. (b) Kohler, N.; Fryxell, G. E.; Zhang, M. *J. Am. Chem. Soc.* **2004**, *126*, 7206.
- (3) (a) Hu, A.; Yee, G. T.; Lin, W. U. *J. Am. Chem. Soc.* **2005**, *127*, 12486. (b) Roucoux, A.; Schulz, J.; Patin, H. *Chem. Rev.* **2002**, *102*, 3757.
- (4) (a) Sun, S.; Murray, C. B.; Weller, D.; Folks, L.; Moser, A. *Science* **2000**, *287*, 1989. (b) Thomson, T.; Toney, M. F.; Raoux, S.; Lee, S. L.; Sun, S.; Murray, C. B.; Terris, B. D. *J. Appl. Phys.* **2004**, *96*, 1197. (c) Wolf, H.; Birringer, R. *J. Appl. Phys.* **2005**, *98*, 074303/1.
- (5) (a) Zhan, C.; Li, D.; Zhang, D.; Xu, W.; Nie, Y.; Zhu, D. *Optical Materials* **2004**, *26*, 11. (b) Qu, S.; Du, C.; Song, Y.; Wang, Y.; Gao, Y.; Liu, S.; Li, Y.; Zhu, D. *Chem. Phys. Lett.* **2002**, *356*, 403. (c) Kityk, I. V.; Ebothe, J.; Fuks-Janczarek, I.; Umar, A. A.; Kobayashi, K.; Oyama, M.; Sahraoui, B. *Nanotechnology* **2005**, *16*, 1687.
- (6) (a) Sun, S.; Zeng, H.; Robinson, D. B.; Raoux, S.; Rice, P. M.; Wang, S. X.; Li, G. *J. Am. Chem. Soc.* **2004**, *126*, 273. (b) O'Connor, C. J.; Sims, J.; Kumbhar, A.; Kolesnichenko, V. L.; Zhou, W. L.; Wiemann, J. A. *J. Magn. Magn. Mater.* **2001**, *226–230* (Pt. 2), 1915.
- (7) (a) Dabbousi, B. O.; Rodriguez-Viejo, J.; Mikulec, F. V.; Heine, J. R.; Mattoussi, H.; Ober, R.; Jensen, K. F.; Bawendi, M. G. *J. Phys. Chem. B* **1997**, *101*, 9463. (b) de Mello Donega, C.; Hickey, S. G.; Wuister, S. F.; Vanmaekelbergh, D.; Meijerink, A. *J. Phys. Chem. B* **2003**, *107*, 489.
- (8) (a) Hostetler, M. J.; Green, S. J.; Stokes, J. J.; Murray, R. W. *J. Am. Chem. Soc.* **1996**, *118*, 4212. (b) Ingram, R. S.; Hostetler, M. J.; Murray, R. W. *J. Am. Chem. Soc.* **1997**, *119*, 9175. (c) Hostetler, M. J.; Templeton, A. C.; Murray, R. W. *Langmuir* **1999**, *15*, 3782.
- (9) Morrison, R. T.; Boyd, R. N. *Organic Chemistry*; 6th ed.; Prentice Hall: Englewood Cliffs, NJ, 1992.
- (10) Carey, F. A.; Sundberg, R. J. *Advanced Organic Chemistry: Part A: Structure and Mechanism*, 3rd ed.; Plenum Press: New York, 1990; p 476.
- (11) Templeton, A. C.; Hostetler, M. J.; Warmoth, E. K.; Chen, S.; Hartshorn, C. M.; Krishnamurthy, V. M.; Forbes, M. D. E.; Murray, R. W. *J. Am. Chem. Soc.* **1998**, *120*, 4845.
- (12) Lwowski, W. In *1,3-Dipolar Cycloaddition Chemistry*; Padwa, A., Ed.; Wiley: New York, 1984.
- (13) Huisgen, R. *Pure Appl. Chem.* **1989**, *61*, 613.

Scheme 1. "Click" Functionalization of Au Nanoparticle Surfaces^a

^a (i) Br(CH₂)₁₁SH in DCM, 60 h at room temperature; (ii) 0.25 M NaN₃ in DCM/DMSO solution, 48 h; (iii) R = propyn-1-one derivatized compounds as in Scheme 2, 24–96 h in dioxane or 1:1 hexane/dioxane.

species react with ethynyl groups to form a 1,2,3-triazole ring.¹⁴ Click chemistry has been extensively applied in organic chemistry¹⁵ and has been recently used to modify electrodes,¹⁶ glass surfaces, and microparticles¹⁷ and to create fluorescent polymer nanospheres.¹⁸ We reasoned that triazole coupling reactions could analogously be utilized as a general method for the functionalization of metal nanoparticle surfaces. This reaction scheme is a particularly powerful approach because only mild reaction conditions are required, and the extreme selectivity toward molecules bearing azides and alkynes prevents unwanted side products.

The general synthetic strategy for triazole functionalization of nanoparticles is shown in Scheme 1. As a model system to demonstrate use of this synthetic approach, we have initially chosen to employ Au nanoparticles because their analysis and characterization using NMR and IR spectroscopies are well-precedented in the literature.¹⁹ This paper describes the synthesis of a series of redox active, fluorescent, and solubilizing species and the use of click chemistry as a facile route toward functionalization of monolayer-protected Au nanoparticles. We demonstrate the ability to link more than one moiety to the particles, paving the way for the creation of chemically useful, multifunctional particles for complex chemical reactions.

Experimental Section

Reagents. 11-Bromo-1-undecanethiol (BrC₁₁H₂₂SH),²⁰ 1-ferrocenyl-2-propyn-1-one (Fc),²¹ 1-(nitrophenyl)-2-propyn-1-one (NB),²²

- (14) (a) Kolb, H. C.; Finn, M. G.; Sharpless, K. B. *Angew. Chem., Int. Ed.* **2001**, *40*, 2004. (b) Rostovtsev, V. V.; Green, L. G.; Fokin, V. V.; Sharpless, K. B. *Angew. Chem., Int. Ed.* **2002**, *41*, 2596.
- (15) (a) Kolb, H. C.; Sharpless, K. B. *DDT* **2003**, *8*, 1128. (b) Lewis, W. G.; Green, L. G.; Grynszpan, F.; Radić, Z.; Carlier, P. R.; Taylor, P.; Finn, M. G.; Sharpless, K. B. *Angew. Chem., Int. Ed.* **2002**, *41*, 1053.
- (16) Collman, J. P.; Devaraj, N. K.; Chidsey, C. E. D. *Langmuir* **2004**, *20*, 1051.
- (17) Lummestorfer, T.; Hoffman, H. *J. Phys. Chem. B* **2004**, *108*, 3963.
- (18) (a) O'Reilly, K. R.; Joralemon, M. J.; Wooley, K. L.; Hawker, C. J. *Chem. Mater.* **2005**, *17*, 5976. (b) Joralemon, M. J.; O'Reilly, K. R.; Hawker, C. J.; Wooley, K. L. *J. Am. Chem. Soc.* **2005**, *127*, 16892.
- (19) Hostetler, M. J.; Wingate, J. E.; Zhong, C.-J.; Harris, J. E.; Vachet, R. W.; Clark, M. R.; Londono, J. D.; Green, S. J.; Stokes, J. J.; Wignall, G. D.; Glush, G. L.; Porter, M. D.; Evans, N. D.; Murray, R. W. *Langmuir* **1998**, *14*, 17.
- (20) Bain, C. D.; Troughton, E. B.; Tao, Y. T.; Evall, J.; Whitesides, G. M.; Nuzzo, R. G. *J. Am. Chem. Soc.* **1989**, *111*, 321.
- (21) Barriga, S.; Marcos, C. F.; Riant, O.; Torroba, T. *Tetrahedron* **2002**, *58*, 9785.
- (22) Pigge, F. C.; Ghasedi, F.; Zheng, Z.; Rath, N. P.; Nichol, G.; Chickos, J. S. *J. Chem. Soc., Perkin Trans. 2* **2000**, 2458.

and propynoyl chloride²³ were synthesized according to literature procedures. Acetonitrile was distilled over CaH₂ prior to use; water was purified with a Barnstead NANOpure system. Tetrabutylammonium hexafluorophosphate was recrystallized three times from ethyl acetate and dried under vacuum at 80 °C. Ethanol (Pharmco), toluene (VWR), dichloromethane (DCM; Fisher), dioxane (ICN Biomedical), dimethyl sulfoxide (DMSO; Alfa Aesar), and all other chemicals were used as received.

Synthesis. *1-Pyrene-1-yl-propyn-1-one (Pyr)*. A 1.02 g (4.44 mmol) amount of pyrene-1-carboxaldehyde was placed in a round-bottom flask under nitrogen. To the flask was added 5 mL of anhydrous tetrahydrofuran (THF), followed by 14 mL of 0.5 M ethynylmagnesium bromide (7 mmol) in THF. The solution was allowed to stir overnight, the reaction was quenched with 20 mL of saturated aqueous ammonium chloride, and the product (pyrene alcohol) was extracted three times with 30 mL of diethyl ether. The combined organic layers were dried over sodium sulfate, and the ether was removed by rotary evaporation. The product was dissolved in 50 mL of anhydrous acetone, and Jones reagent was added dropwise with stirring until a red color persisted. The reaction was quenched with ~3 mL of isopropyl alcohol, changing the solution to a green color. A 50 mL amount of saturated aqueous sodium metabisulfite was added to the flask, and the acetone was removed by rotary evaporation. The product was extracted three times with methylene chloride, and the combined organic layers were dried over sodium sulfate. Purification on a silica column with 1:1 hexanes/ethyl acetate afforded 0.45 g of product (40% yield) as an intense yellow solid. ¹H NMR (CDCl₃, 360 MHz): 3.56 (1H, s), 8.17 (2H, t), 8.26 (3H, d), 8.44 (2H, m), 8.96 (1H, d), 9.50 (1H, d). FTIR (KBr, cm⁻¹): ν 3220 (H—C≡C), 3036 (H—C=C), 2088 (C≡C), 1942, 1917, 1634 (C=O), 1539 (C=C), 1506 (C=C), 1372, 1246, 1221, 1000, 965, 843, 704.

1-Anthracen-9-yl-propyn-1-one (An). Anthracene-9-carboxaldehyde (1.83 g, 8.9 mmol) was placed in a round-bottom flask under nitrogen. A 10 mL amount of anhydrous THF was added, followed by 28 mL of 0.5 M ethynylmagnesium bromide (14 mmol) in THF. The solution was allowed to react for 1 h, was quenched with 20 mL of aqueous saturated ammonium hydroxide, and was allowed to stir overnight. The product, anthracenyl alcohol, was extracted three times with 30 mL of diethyl ether, and the combined organic layers were dried over sodium sulfate. The ether was removed by rotary evaporation, and 53 mL of methylene chloride was added to the resultant red orange product. Activated Mn(IV) oxide (23.2 g, 267 mmol) was added to the solution, and the suspension was stirred for 1.5 h. The product was filtered through Celite and rinsed with methylene chloride until the washings were colorless. The

- (23) (a) Wehler, J.; Feld, W. *J. Chem. Eng. Data* **1989**, *34*, 142. (b) Blush, J.; Park, J.; Chen, P. *J. Am. Chem. Soc.* **1989**, *111*, 8951.

filtrate was concentrated, and the product was purified by silica column chromatography using a gradient elution from 3:1 to 1:1 hexanes/ethyl acetate. Solvent was removed from the desired fraction to afford 1.18 g (52% crude yield) as an intense yellow solid. The product contains inseparable aldehyde impurity and is used without further purification. $^1\text{H NMR}$ (CDCl_3 , 360 MHz): 3.50 (1H, s), 7.48 (4H, m), 7.96 (2H, d), 7.99 (2H, d), 8.50 (1H, s). FTIR (KBr, cm^{-1}): ν 3291 (H—C≡C), 3053 (H—C=C), 2112 (C≡C), 1653 (C=O), 1525 (C=C), 1447 (C=C), 1054, 1028, 916, 891, 790, 733, 638.

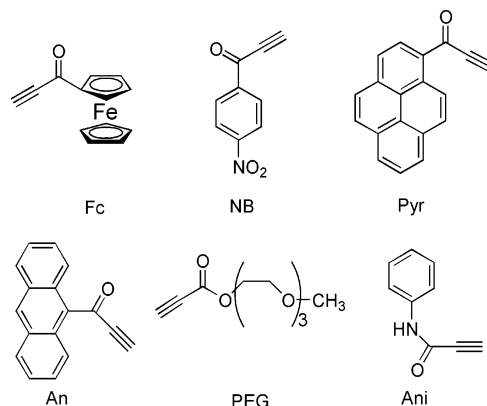
Propynoic Acid 2-[2-(2-Methoxyethoxy)ethoxy]ethyl Ester (PEG). A 20 mL solution containing 2.9 mL (25 mmol) of triethylene glycol monomethyl ether in anhydrous methylene chloride was prepared. To this was added 15 mL of a 1.8 M solution of propynoyl chloride in toluene, and the reaction was stirred overnight. The product was washed three times with 30 mL of water, and the methylene chloride layer was dried over sodium sulfate. The solvent was removed by rotary evaporation to yield a clear colorless oil, which was purified on a silica column using 1:5 acetone/methylene chloride as the eluent. A 0.58 g amount of the pure oil (10.7% yield) was isolated. $^1\text{H NMR}$ (CDCl_3 , 360 MHz): 2.60 (1H, s), 3.28 (3H, s), 3.59 (2H, t), 4.23 (2H, q). FTIR (KBr, cm^{-1}): ν 3220 (H—C≡C), 2144 (C≡C), 1719 (C=O), 1615 (O—C=O), 1456 (—CH₂—), 1352, 1228, 1170, 1108 (C—O—C), 1030, 944, 851, 733.

Propynoic Acid Phenylamide (Ani). A 7.5 mL quantity of a 1.6 M solution of propynoyl chloride in toluene was placed in a round-bottom flask. This solution was diluted with 25 mL of anhydrous methylene chloride and degassed with nitrogen. A 2.2 mL volume (24 mmol) of freshly distilled aniline was added slowly via syringe, and the resultant cloudy yellow reaction mixture was allowed to stir overnight. The resulting solution was washed three times with water, and the organic layer was dried over magnesium sulfate. The solids were removed by filtration, and the solvent was evaporated to give a yellow oil that was purified on a gradient silica column using 3:1 to 1:1 hexanes/ethyl acetate. Collection of the desired fraction and removal of solvent by rotary evaporation yielded 0.62 g (36% yield) of the desired lemon yellow product. $^1\text{H NMR}$ (CDCl_3 , 360 MHz): 2.91 (1H, s), 7.12 (1H, t), 7.33 (2H, t), 7.49 (2H, d), 7.66 (1H, s). FTIR (KBr, cm^{-1}): ν 3393, 3269 (H—C≡C), 3132, 3070 (H—C=C), 2110 (C≡C), 1653 (C=O), 1597 (—C(=O)—N), 1535 (C=C), 1500 (—C(=O)—N), 1442, 1322, 1303, 1268, 1212, 1029, 953, 907, 763, 731, 693, 505.

Au Particle Synthesis and Exchange. Au particles were synthesized according to the two phase method of Brust et al.²⁴ with slight modifications. Briefly, 0.31 g of HAuCl_4 (0.91 mmol) in 10 mL of water was transferred into 80 mL of toluene using 1.5 g of tetraoctylammonium bromide (2.7 mmol). The organic phase was isolated, and 0.47 g of decanethiol (2.7 mmol) was added. The solution was cooled to 0 °C and stirred for 10 min, after which 10 mL of an aqueous solution containing 380 mg of NaBH_4 (10 mmol) was added. This was allowed to stir for an additional 3 h before the organic layer was separated and evaporated, producing a black, waxy solid that was washed with copious amounts of ethanol.

Ligand exchange with $\text{BrC}_{11}\text{H}_{22}\text{SH}$ was performed according to literature methods²⁵ by dissolving 800 mg of synthesized Au nanoparticles and 800 mg of $\text{BrC}_{11}\text{H}_{22}\text{SH}$ in DCM and stirring the solution at room temperature for 60 h. The resulting particles were isolated by evaporation of the solvent, rinsed with ethanol, and dried. Following standard characterization methods,²⁵ the NMR and Fourier transform infrared (FTIR) spectra are consistent with

Scheme 2. Propyn-1-one Compounds for Attachment via Triazole Ring Formation



protective monolayers containing both CH_3 - and Br-terminated ligands.

Synthesis of Azide-Functionalized Au Nanoparticles. The Au- ω -Br-functionalized particles were dissolved in DCM (~ 10 mg/mL) and added to an equal volume of 0.25 M NaN_3 in DMSO. The solution was allowed to stir for 48 h, after which water was added and the black organic layer was isolated. The organic layer was dried over sodium sulfate, the solvent was evaporated, and the particles were washed with ethanol and dried. The particles were subsequently dissolved in dioxane for further use.

Reaction of Azide-Functionalized Au Nanoparticles with Alkynyl Derivatives. In a typical reaction, ~ 50 mg of N_3 -functionalized particles and 0.1 mmol of the alkynyl-modified compound (from Scheme 2) were codissolved in 6 mL of dioxane or 1:1 hexane/dioxane and stirred for 24–96 h. After removing the solvent under vacuum, ethanol was used to remove any unreacted alkynyl derivative, and the particles were dried and then redissolved in DCM. Insoluble material was removed by centrifugation, and the remaining decantate was retained for further analysis.

Particle Decomposition Reactions. Au nanoparticle samples were decomposed using standard disulfide forming reactions,²⁶ in which ~ 3 mg of I_2 was added to ~ 25 mg of particles dissolved in DCM, and the reaction mixture was stirred for 2 h. The resulting black precipitate was removed via centrifugation, and the solution was evaporated to dryness.

Characterization. Transmission Electron Microscopy (TEM). TEM samples were prepared by drop casting a dilute nanoparticle solution in DCM onto copper TEM grids coated with a layer of amorphous carbon. Images were obtained using a JEOL JEM 1200 EXII transmission electron microscope operated at 80 keV and equipped with a Tietz F224 digital camera.

Spectroscopy. $^1\text{H NMR}$ spectra were obtained using either a Bruker AV 360 MHz spectrometer or a Bruker DRX 400 MHz spectrometer using CDCl_3 solutions. Diffuse reflectance infrared spectra were measured with a Varian FTS 7000 using samples drop cast onto powdered KBr. Fluorescence spectra were acquired with a Photon Technology International (PTI) fluorimeter using solutions containing 0.01–0.06 mg/mL particles in filtered, stabilizer free DCM.

Electrochemistry. Cyclic voltammetry was performed with a CH Instruments 600B potentiostat using a 2 mm diameter Pt working electrode, Pt wire counter electrode, and Ag quasi reference electrode. All samples were prepared using a 0.2 M TBAPF₆ toluene/acetonitrile solution (2:1) that had been thoroughly de-

(24) Brust, M.; Walker, M.; Bethell, D.; Schiffrin, D. J.; Whyman, R. J. *Chem. Soc., Chem. Commun.* **1994**, 801.

(25) Templeton, A. C.; Hostetler, M. J.; Kraft, C. T.; Murray, R. W. *J. Am. Chem. Soc.* **1998**, *120*, 1906.

(26) (a) Sun, L.; Crooks, R. M.; Chechik, V. *Chem. Commun.* **2001**, 4, 359. (b) Kim, J.-B.; Bruening, M. L.; Baker, G. L. *J. Am. Chem. Soc.* **2000**, *122*, 7616.

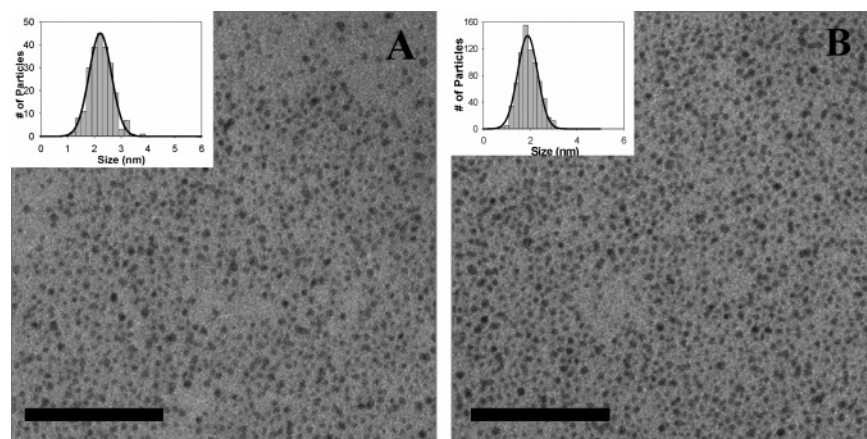


Figure 1. Representative TEM images of (A) as-synthesized C₁₀H₂₁SH-modified Au particles and (B) azide-functionalized Au nanoparticles. Insets contain particle size distributions. Scale bar is 50 nm.

gassed. The electrochemical cell was kept under a blanket of nitrogen for the duration of the experiments. Prior to every run, the working electrode was polished with a 0.05 μm alumina slurry, rinsed with water, sonicated in ethanol, and rinsed with 2:1 toluene/acetonitrile.

Results and Discussion

Azide Functionalization of Au Nanoparticles. To test the functionalization approach shown in Scheme 1, reactions involving triazole ring formation were conducted using small Au particles because of their facile synthesis, solubility, and rapid surface ligand exchange dynamics. We, therefore, synthesized monolayer-protected Au clusters using decanethiol as the surface ligand because this length sufficiently stabilizes the particles from aggregation but is not so sterically hindered as to prevent ligand exchange.^{8c} The synthesized Au nanoparticles, shown in the representative TEM image in Figure 1A, are spherical and have an average diameter of 1.8 ± 0.4 nm. The decanethiol stabilized Au particles were then stirred in a solution containing BrC₁₁H₂₂-SH to replace a fraction of these ligands with Br-terminated undecanethiol ligands. Confirmation of replacement was obtained from the ¹H NMR and FTIR spectra, which were consistent with previous reports of ligand exchange of Au nanoparticles.²⁵ Reaction of the Br termini via nucleophilic substitution with NaN₃ was used to append azide functionalities to the Au nanoparticles. Shown in Figure 1B, the size and shape of the resultant particles are not affected over the course of this reaction.

The FTIR spectrum of the Au nanoparticles after reaction with NaN₃ is compared to that obtained for the as-prepared decanethiol stabilized (i.e., CH₃-terminated) Au nanoparticles to determine the degree of functionalization. The FTIR spectrum of the alkanethiol stabilized particles (Figure 2, solid line) is relatively featureless and contains characteristic alkyl stretching vibrations between 2800 and 3000 cm⁻¹. Consistent with detailed FTIR investigations of monolayer-protected Au clusters,²⁷ the symmetric and antisymmetric vibrational modes at 2850 and 2921 cm⁻¹, respectively, indicate that the alkyl chains are well-ordered and are in a predominately trans orientation. In comparison, the FTIR

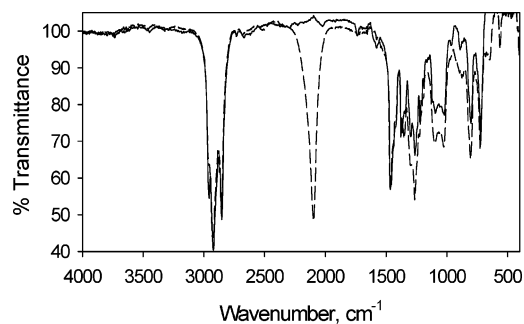


Figure 2. FTIR spectra of the as-synthesized C₁₀H₂₁SH-modified Au particles (solid line) compared to azide-functionalized Au nanoparticles (dashed line).

spectrum of the Au nanoparticles that have been reacted with NaN₃ (Figure 2, dashed line) contains a strong, new vibration centered at 2094 cm⁻¹ that is attributed to the cumulated double bond of the terminal azide moieties. The characteristic alkyl stretching vibrations are not significantly affected (versus the methyl-terminated particles), suggesting that ligand exchange and N₃ substitution do not perturb the structure of the monolayer.

While ¹H NMR spectroscopy of the Au nanoparticles could be used to follow the extent of substitution and reaction of their monolayers, it is well-known that NMR peaks are significantly broadened by attachment to particle surfaces.²⁸ As a result, quantification of ligand exchange can be difficult. An alternative method is to cleave the alkanethiols from the nanoparticles by reaction with I₂ and to subsequently analyze the relative quantities of the solution phase ligands using ¹H NMR spectroscopy. Comparison of the spectra of the ligands obtained from the decomposition of the Au nanoparticles before and after reaction with NaN₃ is shown in Figure 3. The spectrum of the as-prepared particles (Figure 3A) contains triplets at 2.65 and 0.85 ppm that are attributed to the methylenes adjacent to the disulfide and the terminal methyl group, respectively. In contrast, the NMR spectrum of the particles following reaction with NaN₃ (Figure 3B)

(28) (a) Terrill, R. H.; Postlethwaite, T. A.; Chen, C.; Poon, C.-D.; Terzis, A.; Chen, A.; Hutchison, J. E.; Clark, M. R.; Wignall, G.; Londono, J. D.; Superfine, R.; Falvo, M.; Johnson, C. S.; Samulski, E. T.; Murray, R. W. *J. Am. Chem. Soc.* **1995**, *117*, 12537. (b) Badia, A.; Gao, W.; Singh, S.; Demers, L.; Cuccia, L.; Reven, L. *Langmuir* **1996**, *12*, 1262.

(27) Hostetler, M. J.; Stokes, J. J.; Murray, R. W. *Langmuir* **1996**, *12*, 3604.

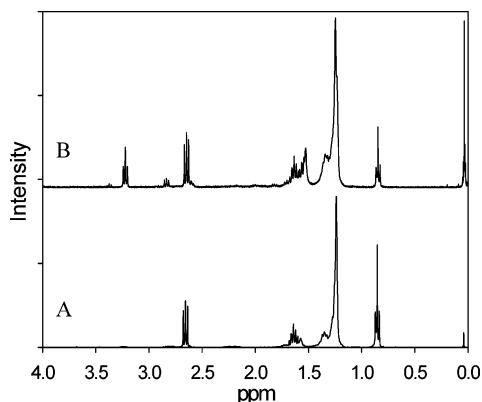


Figure 3. ^1H NMR spectra of solutions containing the products of I_2 decomposition of (A) decanethiol-modified Au nanoparticles and (B) azide-functionalized Au nanoparticles, in CDCl_3 .

contains a new peak at 3.22 ppm that is assigned to the N_3 methylene protons. A small peak at 3.38 ppm, assigned to the Br methylene peak, is also observed; comparison of the integrated areas of the peaks reveals a 92% conversion of Br to N_3 . Taken together, the FTIR and NMR spectra conclusively indicate that ligand replacement with $\text{BrC}_{11}\text{H}_{22}\text{-SH}$ and subsequent reaction with NaN_3 results in Au nanoparticles containing mixed monolayers that are 44% $\text{CH}_3\text{-}$ and 52% $\text{N}_3\text{-}$ terminated alkanethiol ligands.

Triazole Functionalization of Au Nanoparticles. Decorating the nanoparticle surface with N_3 functionalities enables further particle functionalization through 1,3-dipolar cycloaddition reactions (i.e., “click” chemistry) by fusing ethynyl and azide bearing molecules as in Scheme 1. The six different alkynyl compounds shown in Scheme 2, the alkyne derivatives of ferrocene (Fc), nitrobenzene (NB), pyrene (Pyr), anthracene (An), poly(ethylene glycol) (PEG), and aniline (Ani), were synthesized to demonstrate the utility and generality of this method. These reactants were chosen to impart a range of physical, electronic, and spectroscopic properties to the Au nanoparticles. Each was synthesized to include a carbonyl group adjacent to the terminal alkyne to provide a more electron-withdrawing environment that is known to enhance the rate of triazole formation.^{12,16}

Over the course of functionalization, a small amount of precipitation was observed that is most likely a result of minor amounts of particle aggregation. However, the vast majority (>90%) of the material remained soluble and was separated from the insoluble aggregates by centrifugation. Comparison of the TEM images of the soluble Au nanoparticles indicates that there is no appreciable change in their size or morphology (see representative TEM image in Supporting Information) after triazole formation with each of the alkynyl compounds.

We acquired FTIR spectra of the Au nanoparticles to monitor the extent of attachment of the alkynyl compounds; examples of these spectra following reaction with each of the six compounds are shown in Figure 4. In general, reaction of the N_3 -modified particles with the propyn-1-one species results in the formation of several new peaks in the 1600–1800 cm^{-1} region that are attributed to the $\text{C}=\text{O}$ symmetrical stretching vibration. Universally absent from these spectra is the peak at $\sim 3300\text{ cm}^{-1}$ due to the $\text{H}-\text{C}\equiv\text{C}$ stretching

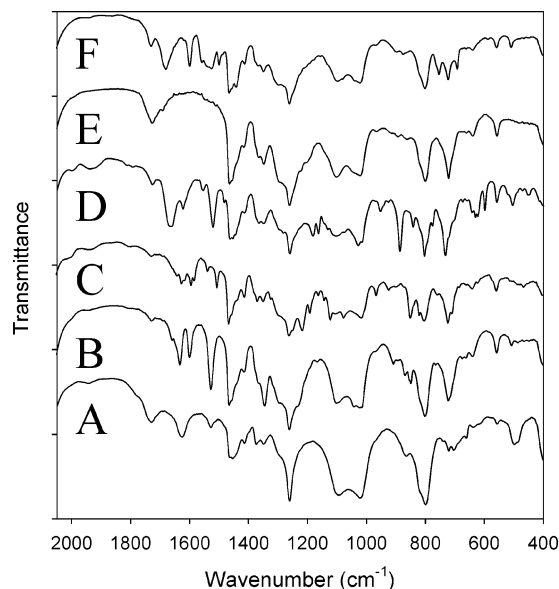


Figure 4. FTIR spectra of Au particles following reaction with the alkynyl-modified compounds: (A) Fc; (B) NB; (C) Pyr; (D) An; (E) PEG; and (F) Ani. Spectra are offset for clarity.

mode (not shown). All of the remaining peaks in the FTIR spectra of the functionalized nanoparticles are consistent with those obtained for their small molecule analogues, suggesting that other than the ring formation, the structures of the compounds are not drastically affected upon surface attachment. In addition, the alkyl stretching vibrations of the alkanethiolate remain unchanged by cycloaddition, indicating that the protecting surface monolayer is largely unaffected by triazole ring formation. Together, these data imply a complete reaction of the triple bond with the terminal N_3 groups on the Au nanoparticles to form a triazole ring and rule out binding by intercalation of the ligand into the particle surface monolayer or the possibility of unreacted alkynyl compounds present as impurities.

To assess the extent of particle functionalization via cycloaddition, we again turned to I_2 decomposition and NMR spectroscopy of the liberated ligands. Upon triazole ring formation, the ligands produce NMR signals that are readily distinguished from the unreacted alkynyl compounds. Although the proton peak intensities are weak because of the relatively small number of protons in comparison with the alkyl protons (not shown, see Supporting Information), the ^1H NMR spectra for Au nanoparticle samples following reaction with each of the six click compounds correspond well with those of the small molecule analogues.

Cycloaddition reactions can also be utilized to prepare multifunctional Au nanoparticles by simultaneously stirring the N_3 -terminated nanoparticles with several acetylenic small molecules. To demonstrate this, we reacted $\text{N}_3\text{-}$ containing Au nanoparticles with a solution containing both the Fc and the NB propyn-1-one species. The FTIR spectrum of the resultant particles is shown in Figure 5A and, analogously to the spectra above (Figure 4), contains vibrations between 1500 and 1700 cm^{-1} due to $\text{C}=\text{O}$ and triazole ring stretching modes. Although it is complex, the spectrum contains the expected transitions for a multifunctional Au nanoparticle containing both Fc and NB species linked through triazole ring formation. Analysis of the composition of the mixed

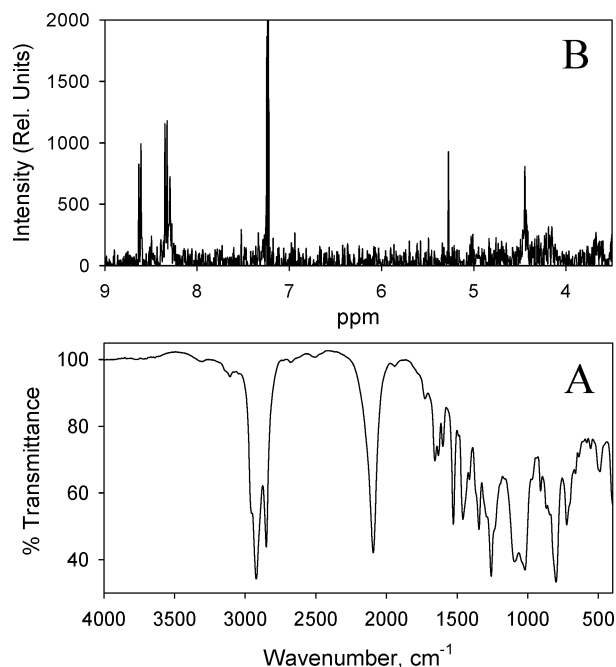


Figure 5. (A) FTIR spectra of Au nanoparticles following reaction with both Fc and NB alkynyl derivatives and (B) ^1H NMR of the CDCl_3 solution containing the products of I_2 decomposition of the particle sample.

monolayer was again accomplished by cleaving the ligands from the particles with I_2 and collecting the ^1H NMR spectra shown in Figure 5B. Two distinct sets of peaks are observed: the broad peak at 4.45 ppm is attributed to the attached Fc units, while those located at 8.4 and 8.6 ppm are due to NB.

Quantitative Assessment of Extent of Functionalization.

Comparison of the peak integrations from the NMR spectra as a function of reaction enables an estimation of the percentages of surface-bound ligands per Au nanoparticle, following a method that has been previously described.¹⁹ Assuming that (a) no ligands are destroyed through side reactions and (b) all ligands are completely cleaved from the surface upon reaction with I_2 , the intensities of the peaks in the NMR spectra are proportional to their relative concentrations on the Au nanoparticles' surfaces. Analysis of peak integrations in Figure 3 for the N_3 -terminated particles reveals that there are ~ 1.2 N_3 -terminated thiols for every CH_3 -terminated thiol. A small peak observed for Br-terminated undecanethiol corresponds to an average of $\sim 4\%$ ligands per particle that are not converted to N_3 upon reaction with NaN_3 . Similar analysis of the NMR spectra of the Au nanoparticles following reaction with the click compounds enables determination of the efficacy of triazole formation. In Table 1, the relative percentages of ligands in the Au nanoparticle monolayer following 60 h of reaction in dioxane for each of the reactants in Scheme 2 are compared. Under identical reaction conditions, the Pyr moiety couples more effectively (13% coupling efficiency) than the other acetylene-derivatized compounds, and the PEG chain is least reactive (1% coupling efficiency). There is no apparent trend with respect to size or reactivity for these compounds; a possible explanation for this variation is a difference in the degree of solvation of the reactants.

Table 1. Relative Composition and Reaction of Au Nanoparticle Monolayers Following "Click" Reactions

cmpd	ω -termini	% lig-ands ^b	% con-version ^c	cmpd	ω -termini	% lig-ands ^b	% con-version ^c
Dioxane ^a							
Fc	CH_3	54	12	An	CH_3	46	6
	N_3	41			N_3	50	
	Fc	6			An	4	
NB	CH_3	44	6	PEG	CH_3	48	1
	N_3	53			N_3	51	
	NB	3			PEG	1	
Pyr	CH_3	44	7	Ani	CH_3	50	6
	N_3	49			N_3	47	
	Pyr	7			Ani	3	
Dioxane/Hexane ^d							
Fc	CH_3	53	22	An	CH_3	47	54
	N_3	37			N_3	25	
	Fc	10			An	28	
NB	CH_3	43	13	PEG	CH_3	48	5
	N_3	49			N_3	50	
	NB	7			PEG	2	
Pyr	CH_3	45	9	Ani	CH_3	50	14
	N_3	46			N_3	43	
	Pyr	9			Ani	7	

^a Reaction at room temperature for 60 h in dioxane. ^b From analysis of the NMR spectra, the percentage of ligands in the Au nanoparticle monolayer. ^c From analysis of the NMR spectra, the percentage of azide moieties that reacted to form triazole rings. ^d Reaction at room temperature for 60 h in a dioxane/hexane (50:50) solution.

Thus, to test the role of solvent on the extent of functionalization, we repeated these reactions in a range of solvents and solvent mixtures. Although polar solvents are often used for triazole ring formation, we observed that the Au nanoparticles were not stable in solutions containing polar solvents (i.e., THF/ H_2O and DCM/EtOH) and precipitated over the course of the reaction. Comparison of reactivity in a series of nonpolar organic solvents (DCM, THF, refluxing ether, and dioxane) for a 24 h reaction period showed that dioxane solutions had the highest yield. No reaction was observed for DCM solutions at this time scale. Complete (100%) conversion of the N_3 groups was never observed with any of the tested solvent systems, even over time periods as long as 96 h, although conversion percentage increased as a function of time.

We reasoned that solubility was a primary factor in determining reactivity and observed that solutions containing both hexane and dioxane would solubilize both the Au nanoparticles and click compounds. The percentage conversion using a 1:1 hexane/dioxane mixture is also compared to pure dioxane solutions in Table 1. For each click compound studied, addition of the more nonpolar (hexane) solvent resulted in an average threefold increase in the efficiency of the azide conversion to triazole. These results are consistent with prior reports, in which hydrophobic solvents better stabilize the nonpolar transition state.²⁹ It is also possible that this effect arises from better solubilization of the hydrophobic monolayer on the Au nanoparticle surfaces by addition of the nonpolar hexane to solution.

Because it has been shown that Cu catalysts can greatly enhance the rate of triazole formation, particularly in aqueous solutions,¹⁴ we also sought to increase the conversion

(29) (a) Rispeers, T.; Engberts, J. B. F. *N. J. Phys. Org. Chem.* **2005**, *18*, 908. (b) Gajewski, J. J. *Acc. Chem. Res.* **1997**, *30*, 219.

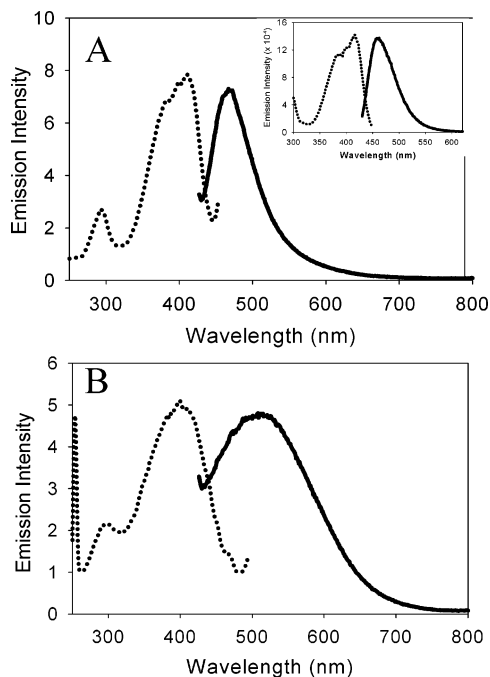


Figure 6. Fluorescence excitation (dotted line, $\lambda_{\text{em}} = \lambda_{\text{max}}$) and emission (solid line, $\lambda_{\text{ex}} = 412$ nm) spectra of (A) Pyr-functionalized and (B) Pyr and Fc bifunctional Au nanoparticles. All solutions were ~ 0.02 mg/mL of Au particles in DCM. Inset contains fluorescence emission and excitation spectra of the propyn-1-one derivative of Pyr.

percentage by employing several different catalyst systems. However, the hydrophobicity of the monolayer-protected particles made them insoluble in aqueous solutions and prevented the use of the most commonly employed CuSO_4 –ascorbic acid system. We, therefore, attempted to use several organic soluble catalysts, including CuI ,³⁰ bromotris(triphenylphosphinato) copper(I),³¹ and $\text{CuBr}/2,6$ -lutidine,³² and in all cases immediate and extensive particle aggregation or decomposition was observed. Our ongoing investigations continue to seek catalysts to improve triazole conversion rates; however, the lower yields may enable the careful control over extent of reaction.

“Clicked” Functionality on Au Nanoparticles. The use of triazole ring formation is a general method by which chemical, spectroscopic, or electrochemical functionality may be appended to metal nanoparticles. We specifically chose the compounds in Scheme 2 to impart unique physical properties to the Au particles. For example, pyrene is a common fluorophore that has been linked to metal nanoparticles; the fluorescence emission and excitation spectra of the modified propyn-1-one Pyr small molecule are shown in the inset of Figure 6A. The emission spectrum of the pyrene small molecule contains a broad peak at 460 nm; when this molecule is linked to Au nanoparticles by formation of the triazole ring, the fluorescence emission maximum appears at 467 nm (Figure 6A). The slight red shift of the fluorescence peak is attributed to an increase in conjugation upon formation of the triazole ring, because the

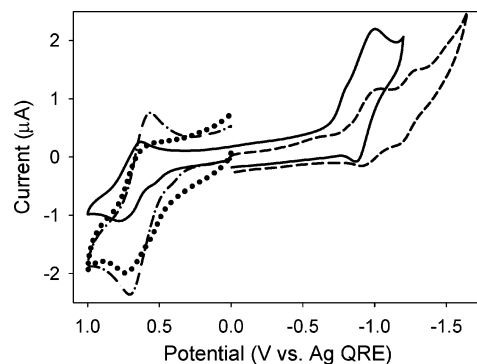


Figure 7. Cyclic voltammetry of Fc- (dashed dotted line); NB- (dashed line); Fc and NB- (solid line); and Fc and Pyr- (dotted line) functionalized Au nanoparticles (~ 2 mg/mL) in a 0.2 M TBAPF_6 solution of 2:1 toluene/acetonitrile. All scans were performed at a potential scan rate of 20 mV/s using a 2 mm diameter Pt working electrode, Pt wire counter electrode, and a Ag quasi reference electrode.

number of pyrenes per particle is so small that their coupling or aggregation is unlikely.

Shown in Figure 6B are the fluorescence emission and excitation spectra obtained using a Au nanoparticle sample which contained both Fc and Pyr attached species. Fluorescence is again observed from the Pyr groups; however, the emission peak is significantly broadened, and the maximum is red-shifted by 50 nm compared to the spectrum in Figure 6A. These effects on the emission spectra may be a result of weak coupling between the pendant Fc and Pyr groups that quenches the Pyr emission, similar to prior observations on glass surfaces.³³ The sensitivity of the Pyr emission peak to the presence of other attached species is potentially important for sensing applications and is the subject of our ongoing studies.

Analogous to literature reports for place-exchanged Au nanoparticles,³⁴ voltammetric methods were also used to confirm triazole ring formation on functionalized Au nanoparticles. Among the reactants in Scheme 2, both Fc and NB are electroactive so that Au nanoparticles reacted with these compounds were examined by cyclic voltammetry. Figure 7 contains representative cyclic voltammograms of Au nanoparticles containing either Fc or NB moieties. In these, the anodic wave at +0.6 V is a result of the one-electron oxidation of attached Fc species; the reductive scan contains two dominant peaks that correspond to sequential one electron reductions of the pendant NB molecules. In the case of the NB-modified particles, the relatively larger current of the forward versus the reverse scan is a result of chemical irreversibility that may be due to particle or ligand decomposition. For the Au nanoparticles containing both Fc and NB, the differences in peak potentials for the forward and reverse scans (ΔE_p) are greater than 59 mV so that the reactions are electrochemically quasi-reversible.³⁵ These results are consistent with previous reports of the voltammetry of redox-modified Au nanoclusters, implying that triazole functionalization does not appreciably affect the

(30) Billing, J. F.; Nilsson, U. J. *J. Org. Chem.* **2005**, *70*, 4847–4850.

(31) Wu, P.; Feldman, A. K.; Nugent, A. K.; Hawker, C. J.; Scheel, A.; Voit, B.; Pyun, J.; Frechet, J. M. J.; Sharpless, K. B.; Fokin, V. V. *Angew. Chem., Int. Ed.* **2004**, *43*, 3928–3932.

(32) Van Maarseveen, J. H.; Horne, W. S.; Ghadiri, M. R. *Org. Lett.* **2005**, *7*, 4503–4506.

(33) Mazur, M.; Blanchard, G. J. *J. Phys. Chem. B* **2005**, *109*, 4076.

(34) (a) Green, S. J.; Pietron, J. J.; Stokes, J. J.; Hostetler, M. J.; Vu, H.; Wuelfing, P.; Murray, R. W. *Langmuir* **1998**, *14*, 5612. (b) Miles, D. T.; Murray, R. W. *Anal. Chem.* **2001**, *73*, 921.

(35) Bard, A. J.; Faulkner, L. R. *Electrochemical Methods: Fundamentals and Applications*, 2nd ed.; John Wiley & Sons: New York, 2001.

voltammetric behavior of the functionalized particles. Also shown in Figure 7 are voltammograms of Au nanoparticles with mixed monolayers of NB/Fc and Pyr/Fc. In each case, quasi-reversible waves are observed that correspond to the redox reactions for each of the attached species. The voltammograms also contain small prewaves for both the Fc and NB reactions, which are indicative of partial particle adsorption to the electrode surface.³⁶ Together, these experiments demonstrate the ability to append multiple electron donor and acceptor species in a single functionalization step,

(36) Yamada, M.; Tadera, T.; Kubo, K.; Nishihara, H. *J. Phys. Chem. B* **2003**, *107*, 3703.

serving as models for the creation of multifunctional nanoscale particles.

Acknowledgment. This work was supported by grants from American Chemical Society PRF (37553-G4) and National Science Foundation CAREER Award (CHE0239-702).

Supporting Information Available: ¹H NMR spectra of the triazole-functionalized Au nanoparticles and representative TEM images of Au nanoparticles after functionalization with Fc propyn-1-one (PDF). This material is available free of charge via the Internet at <http://pubs.acs.org>.

CM060157B